AIP Journal of Applied Physics

Controlling alloy composition of InAsP self-assembled quantum dots embedded in GaAs

R. L. Maltez, E. Ribeiro, W. Carvalho Jr., D. Ugarte, and G. Medeiros-Ribeiro

Citation: Journal of Applied Physics **94**, 3051 (2003); doi: 10.1063/1.1597762
View online: http://dx.doi.org/10.1063/1.1597762
View Table of Contents: http://scitation.aip.org/content/aip/journal/jap/94/5?ver=pdfcov
Published by the AIP Publishing

Re-register for Table of Content Alerts

Create a profile.
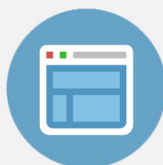
Sign up today!

[This article is copyrighted as indicated in the article. Reuse of AIP content is subject to the terms at: http://scitation.aip.org/termsconditions. Downloaded to] IP: 200.130.19.173 On: Wed, 19 Mar 2014 16:22:22

JOURNAL OF APPLIED PHYSICS VOLUME 94, NUMBER 5 1 SEPTEMBER 2003

Controlling alloy composition of InAsP self-assembled quantum dots embedded in GaAs

R. L. Maltez,[a] E. Ribeiro, W. Carvalho, Jr., D. Ugarte, and G. Medeiros-Ribeiro
Laboratório Nacional de Luz Síncrotron, Caixa Postal 6192, 13084-971 Campinas-SP, Brazil

(Received 3 February 2003; accepted 10 June 2003)

We report on the growth of quantum dot (QD) layers of InAsP alloys buried in GaAs by low-pressure metalorganic chemical vapor deposition. Ternary QDs were obtained by the addition of a PH_3 flux during the InAs QD growth, exhibiting recombination energies lying between those of InAs and InP QDs. The electronic properties of these QDs, as evaluated by photoluminescence spectroscopy, could be tailored by varying both the growth rate and the PH_3 flux for a constant AsH_3 flux. The morphology of these QDs was investigated by transmission electron microscopy from which the formation of an InAsP ternary alloy QDs was inferred. Based on electron microscopy results, the fundamental role of As incorporation on the morphology of and on the defect nucleation associated to InAsP QDs could be then evaluated. From this optical–structural combined analysis, we were able to identify the growth conditions that produce good quality InAsP QDs embedded in GaAs. © *2003 American Institute of Physics.* [DOI: 10.1063/1.1597762]

I. INTRODUCTION

Self-assembled quantum dots (QDs) epitaxially grown on lattice-mismatched substrates have received a lot of attention in the recent years as a prototypical system for the implementation of zero-dimensional structures.[1,2] The usual choice of materials for the formation of QDs concentrated mainly in the III–V and II–VI semiconducting compounds, due to their direct gap and consequently, their optoelectronic application potential. Nevertheless, the growth of group-IV semiconducting islands has provided a great deal of information insofar as the growth thermodynamic and kinetic processes are concerned. These turn out to be extremely important should one desire to tune the electronic properties of QDs by changing their size and shape.

Another approach to tuning QD electronic properties is to use ternary alloys for the island material. By varying the alloy composition, one can modify both the structural and electronic properties of QDs. Ternary $III_xIII_{1-x}V$ QDs, such as InGaAs/GaAs (Refs. 3 and 4) or InAlAs/AlGaAs (Refs. 4 and 5) have been studied extensively, as the stoichiometry is considerably easier to control due to the fact that the incorporation of cations is nearly 100%, regardless of the growth technique used. For metalorganic chemical vapor deposition (MOCVD), the mixing in the cation sublattice is determined by the rate of mass transport of each group-III element to the surface. In the case of InGaAs, re-evaporation of In, of course, will change the distribution coefficient k, defined as the ratio of the concentration of cations A and B in the solid divided by that in vapor. In any case, for most practical growth conditions, k is about 1, which makes the stoichiometry easier to control. The stoichiometry of $IIIV_xV_{1-x}$ alloys is considerably more complicated, due to the higher volatility of group-V elements. In addition to that, the incomplete pyrolisis of the anion source molecules will complicate the analysis, especially at lower temperatures. Thus, the study of Stranskii–Krastanow (SK)-grown $IIIV_xV_{1-x}$ alloys to produce islands on GaAs has been marginally addressed so far and, in fact, there are limited reports on the use of these materials for the formation of QDs.[6,7] In one report, Vinokurov *et al.*[7] attempted the growth of InP/InGaP and InAsP/InGaP QDs. The ternary alloy QDs exhibited no appreciable photoluminescence (PL) energy shift when compared to the InP/InGaP QD emission. This is somewhat surprising, as PH_3 is more stable than AsH_3. Nevertheless, strain, as well as catalytic effects, might also play a role in the As incorporation in self-assembled islands.

The importance of the growth of InAsP QDs is twofold: (1) the possibility of controlling the luminescence emission in QDs, as both ends of the alloy will inevitably grow in the SK mode, and (2) the possibility of tuning the g factor in low-dimensional structures, which will have important consequences in the implementation of quantum communication devices.[8] In addition to these possibilities, we have also to consider that the system InAsP in GaAs will undergo a type I to type II band line up,[9] which may allow some control of recombination time. Finally, the ability of controlling the mixing in the anion sublattice of strained layers is of fundamental importance as well, and SK islands are an interesting prototypical system, as the amount of strain can be substantial. It was already shown that it is possible to tune the luminescence PL energy by using the InAsP alloy.[10] Here, we present a detailed study aimed at understanding the influence of the growth parameters on the ternary QDs formation. We performed several growth experiments targeted at controlling As incorporation into QDs, by varying the anion partial pressure as well as the growth rate. We investigated the grown structures by transmission electron microscopy (TEM) and PL spectroscopy techniques. We were able to show that ternary alloy QDs can be grown with properties that lie be-

[a]Permanent address: Instituto de Física, Universidade Federal do Rio Grande do Sul, Caixa Postal 15051, 91501-970 Porto Alegre-RS, Brazil.

 © 2003 American Institute of Physics

[This article is copyrighted as indicated in the article. Reuse of AIP content is subject to the terms at: http://scitation.aip.org/termsconditions. Downloaded to] IP: 200.130.19.173 On: Wed, 19 Mar 2014 16:22:22

tween those of InAs and InP QDs. In particular, we were able to infer that the equilibrium shape of the QD changes as more As is incorporated into the islands.

II. EXPERIMENTAL DETAILS

The samples were grown on a commercial MOCVD reactor operating at 70 Torr under a H_2 flow of 12 l/min, using trimethilindium, triethilgallium, phosphine (PH_3), and arsine (AsH_3) as precursors. A 300 nm thick GaAs buffer layer was grown on GaAs:Cr (001) substrates, followed by the deposition of the QD layer (InAs, InAsP, or InP). The dots were annealed under the H_2 flux for 60 s (except for the InP samples) and then covered by a 60 nm thick GaAs capping layer. The growth temperature T_g was 640 °C for the GaAs buffer and 550 °C for the remaining layers. The deposited material coverage was 2.1 monolayers (ML) for InAs, near the coherence/incoherence transition for island growth, and 4 ML for the remaining samples. The AsH_3 flux was kept constant at 0.8 standard cubic centimeter per minute (sccm) for the InAs and InAsP QD samples, and the ternary QDs were obtained by the addition of a PH_3 flux during the InAs QD growth. The ternary alloy composition was varied by changing the growth rate g_r (from 0.1 to 0.4 ML/s) and the PH_3 flux (5 and 10 sccm).

PL experiments were performed at 77 K (liquid-nitrogen immersion cryostat) using the 5145 Å line of an Ar^+ laser as excitation source. The power density varied from 1.5 to 400 W/cm^2. The PL emission was dispersed by a 0.75 m single spectrometer and detected by a cooled Ge photodiode. Cross-sectional and plan-view TEM micrographs were taken using an atomic resolution JEOL JEM-3010 URP microscope operating at 300 kV of acceleration voltage. Specimens were prepared by mechanical polishing and dimpling, followed by ion milling using a nitrogen-cooled stage.

III. RESULTS AND DISCUSSION

Figure 1 presents a global map of the QD samples included in this study,[10] by plotting their PL peak positions as a function of the growth rate. The binary InAs and InP QDs are represented by solid circles and squares in Fig. 1, and the ternary InAsP QDs by open diamonds. The PH_3 fluxes used to obtain the InAsP QDs are indicated next to the data. From Fig. 1, it can be seen that all the InAsP QDs have emission energies that lie between those of the binary islands, as expected. Also, regarding the ternary islands, for $g_r = 0.1$ ML/s it was impossible to obtain emission energies below 1.28 eV, even for the lowest measurable PH_3 flux. However, by increasing g_r, the InAsP QD emission gradually shifts to the red,[10] indicating that the As incorporation is becoming more efficient. Although the PL results are consistent with the formation of InAsP QDs, we cannot rule out that smaller InAs QDs (or bigger InP QDs) could be responsible for the PL spectra of our ternary QDs (diamonds in Fig. 1). The emission redshift for increasing g_r could also be a consequence of QD size variations. In this light, a TEM study of selected samples is fundamental to substantiate the assumption of InAsP QDs formation and to monitor the island morphology evolution as a function of the growth conditions. In the following sections, we will present a TEM analysis of two subgroups of samples: (i) a set where g_r and the AsH_3 were kept constant, while varying the PH_3 flux, and another set (ii) where the growth rate was varied while keeping both AsH_3 and PH_3 fluxes constant. The amount of deposited material was the same for all samples, fixed nominally at 4 ML, except for the InAs samples, where it was kept at 2.1 ML.

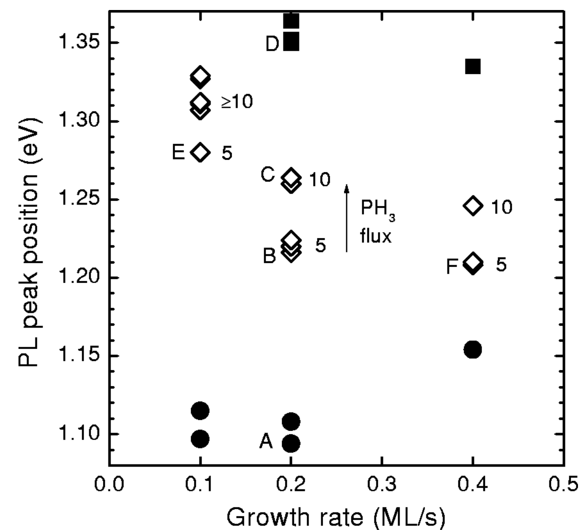

FIG. 1. PL peak position as a function of the growth rate for the QD samples grown for the present study: InAs (filled circles), InAsP (open diamonds), and InP (filled squares). The numbers placed close to the InAsP points indicate the PH_3 flux used during their respective growths. Labels indicate samples A through F.

A. Varying the PH_3 flux

Figure 2 shows plan-view micrographs taken under two beam condition with **g** = 220 for samples A to D, respectively: [Fig. 2(a)] Pure InAs QDs; [Figs. 2(b) and 2(c)] expected to be nominally InAsP QDs; and [Fig. 2(d)] pure InP QDs (see Fig. 1). The growth rate was fixed to $g_r = 0.2$ ML/s for all these samples and the PH_3 flux was decreased from sample C to B in order to increase the distribution coefficient for As and, therefore, lower the emission energy. From these images, we determined the dot density for each sample, all lying in the range of 10^{10} dots/cm^2 (Table I). In addition, samples A through C presented the nucleation of some defective islands, about one order of magnitude lower in number density than the defect-free islands (Table I). The nucleation of defective islands was somewhat anticipated, as the amount of deposited material was near the coherence–incoherence transition for island growth: some of the islands grew beyond a critical size and the introduction of defects occurred.[11] The InP QDs (sample D), on the other hand, showed no defective islands on the whole analyzed area.

The most important result from the plan-view images in Fig. 2 is a monotonic trend for the QD average diameters of samples A through D. It can be better visualized in Fig. 3, where we present cross-sectional TEM micrographs taken under the dark-field 002 (DF 002) imaging condition for the same set of samples. In these images, the islands have a

[This article is copyrighted as indicated in the article. Reuse of AIP content is subject to the terms at: http://scitation.aip.org/termsconditions. Downloaded to] IP: 200.130.19.173 On: Wed, 19 Mar 2014 16:22:22

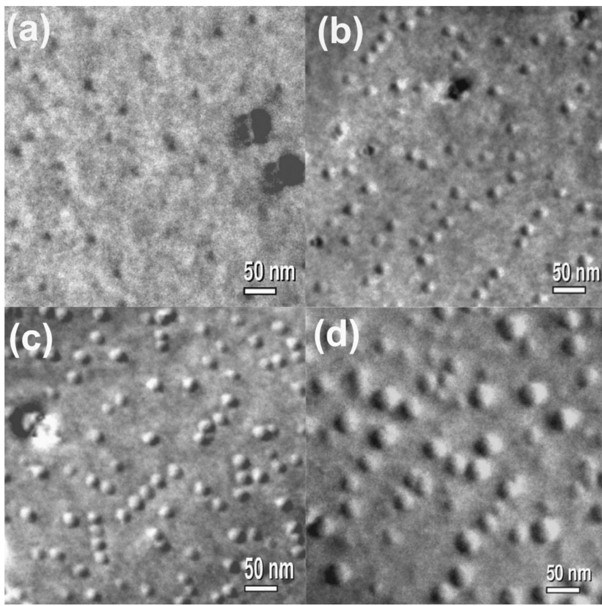

FIG. 2. (a)–(d) Plan-view micrographs taken under two beam condition with **g**=220 of samples A (InAs), B and C (InAsP), and D (InP), respectively. g_r was kept fixed at 0.2 ML/s; samples B and C were obtained using a PH_3 flux of 5 and 10 sccm. The dot densities are: (a) (2.3 ± 0.5) 10^{10} dots/cm_2, (b) (4.1 ± 0.3) 10^{10} dots/cm^2, (c) (4.3 ± 0.3) 10^{10} dots/cm^2, and (d) (3.0 ± 0.3) 10^{10} dots/cm^2.

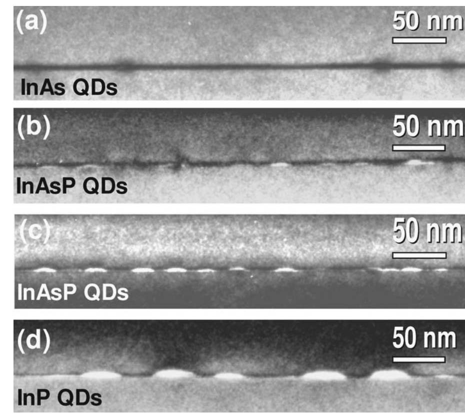

FIG. 3. (a)–(d) Cross-sectional TEM DF 002 micrographs of samples A (InAs), B and C (InAsP), and D (InP), respectively. g_r was kept fixed at 0.2 ML/s; samples B and C were obtained using a PH_3 flux of 5 and 10 sccm. The average dot diameters are: (a) (13 ± 2) nm, (b) (15 ± 3) nm, (c) (20 ± 5) nm, and (d) (32 ± 6) nm.

white contrast, except for the InAs QDs [Fig. 3(a)], where the contrast is not clearly defined. The QD diameters are $d_A=(13\pm2)$ nm, $d_B=(15\pm3)$ nm, $d_C=(20\pm5)$ nm, and $d_D=(32\pm6)$ nm, values obtained from averaging several images similar to those in Fig. 3 and high-resolution cross-sectional TEM micrographs (to be discussed later). Since the island heights are approximately the same within experimental error (see Table II), this monotonic trend is a direct evidence of the formation of a ternary alloy in samples B and C, because the island equilibrium size L depends inversely on the strain ε squared ($L\propto\varepsilon^{-2}$).[12] Thus, from InAs (7.2% lattice mismatch to GaAs) to InP (3.8%), the island size should increase, as observed in Figs. 3(a) and 3(d). By Vegard's law, the ternary alloy should have an equilibrium lattice parameter which depends linearly on the composition. Therefore, the InAsP QDs should present lateral dimensions intermediate between those of InAs and InP QDs. Figures 2(b) and 2(c), as well as Figs. 3(b) and 3(c), clearly validate this trend, confirming the formation of the ternary InAsP QDs.

In order to correlate the TEM and the PL data, in Fig. 4, we plot the QD diameter as a function of the PL peak energy. The dotted line is a guide for the eyes and the inset of Fig. 4 displays the PL spectra of samples A through D. Again, a monotonic trend is found: the QD diameter increases with their emission energy. In other words, samples B and C cannot contain binary InAs QDs because this would necessarily lead to a redshift in their recombination energies. This independent evidence further confirms the formation of ternary InAsP dots embedded in GaAs.

B. Varying the growth rate

By varying the growth rate, one can change the growth conditions from thermodynamic to kinetically driven. It was shown in Fig. 1 and the previous section that even for arbitrarily low values of PH_3 fluxes, no efficient As incorporation was found. In a related experiment (not presented here), by doubling the AsH_3 flux, we did not succeed in producing good quality films. One of the reasons for not increasing it further also included the fact that for higher AsH_3 partial pressure, one obtains lower QD densities.[4,13] Therefore, we were limited by that constraint, and in an effort to probe the kinetic aspects of As incorporation, we chose to vary the growth rate.

Figure 5 shows plan-view micrographs taken under two beam condition with **g**=220 of samples E, B, and F (InAsP

TABLE I. Sample identification, QD material, growth rate, PH_3 flux, average dot density, and average defective-dot density (from TEM) for selected samples of the present work. The error bars were assumed to be the mean dispersion.

Sample	Material	g_r (ML/s)	PH_3 flux (sccm)	Dot density (10^{10} dots/cm^2)	Defective dot density (10^{10} dots/cm^2)
A	InAs	0.2	⋯	(2.3 ± 0.5)	(0.17 ± 0.03)
B	InAsP	0.2	5	(4.1 ± 0.3)	(0.19 ± 0.05)
C	InAsP	0.2	10	(4.3 ± 0.3)	(0.15 ± 0.02)
D	InP	0.2	10	(3.0 ± 0.3)	(0)
E	InAsP	0.1	5	(2.3 ± 0.2)	(0.06 ± 0.01)
F	InAsP	0.4	5	(1.3 ± 0.1)	(0.61 ± 0.03)

[This article is copyrighted as indicated in the article. Reuse of AIP content is subject to the terms at: http://scitation.aip.org/termsconditions. Downloaded to] IP: 200.130.19.173 On: Wed, 19 Mar 2014 16:22:22

TABLE II. Sample identification, average dot diameter, and average dot height (from TEM), and calculated island aspect ratio for selected samples of the present work.

Sample	Average dot diameter (nm)	Average dot height (nm)	Aspect ratio
A	(13 ± 2)	(3.6 ± 0.6)	3.6
B	(15 ± 3)	(2.6 ± 0.5)	5.8
C	(20 ± 5)	(2.9 ± 0.7)	6.9
D	(32 ± 6)	(4 ± 1)	8.0
E	(17 ± 5)	(2.7 ± 0.5)	6.3
F	(12 ± 4)	(2.8 ± 0.6)	4.3

QDs, Fig. 1), grown with the PH_3 flux fixed at 5 sccm and the following growth rates: [Fig. 5(a)] $g_r=0.1$ ML/s, [Fig. 5(b)] $g_r=0.2$ ML/s, and [Fig. 5(c)] $g_r=0.4$ ML/s. The presence of defective islands can be readily seen on these images, identified by the asymmetric, large dark spots, most noticeable in Fig. 5(c). Nondefective islands show the conventional black–white contrast due to the strain field of small inclusions. The density of defective islands increased with the growth rate g_r from about 0.5% of the total island density in sample B to almost 50% in sample F (see Table I). The critical layer thickness for the coherent to incoherent transition for island growth depends on the lattice mismatch.[11] Thus, for a constant coverage, the defective island density should increase with the strain. Therefore, we can conclude that the increase of the defective island density is directly related to the increase in As incorporation. Another observation that can be made in Fig. 5 is that the size of the coherent islands for samples E and B [Figs. 5(a) and 5(b)] is about the same, whereas for sample F their size decreases noticeably. This is a further indication that the smaller coherent islands have higher As concentrations, and that correlates well with the increase of the defective island density.

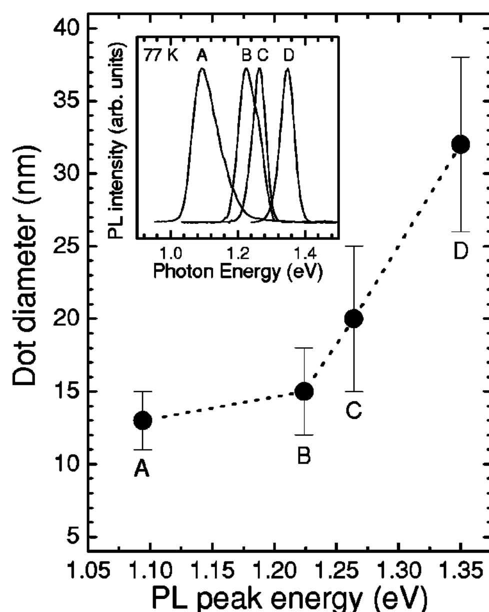

FIG. 4. Average dot diameter as a function of the PL peak energy for samples A through D. Their PL spectra are depicted in the inset. The dotted line is a guide for the eyes.

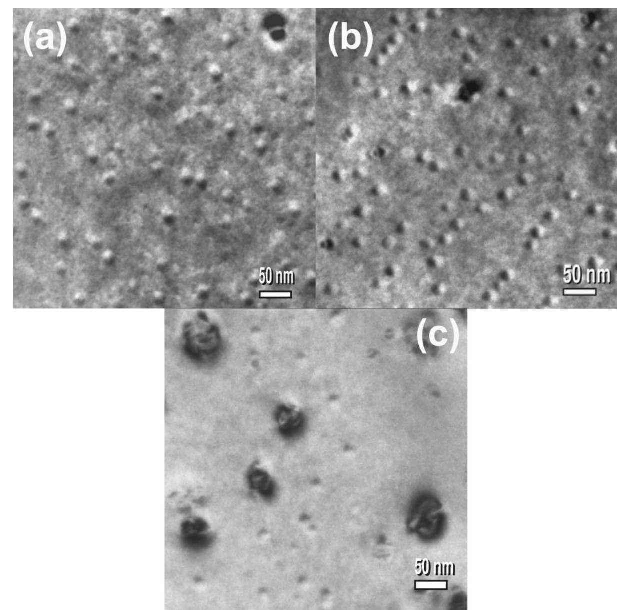

FIG. 5. (a)–(c) Plan-view micrographs taken under two beam condition with $\mathbf{g}=220$ of samples E, B, and F (ternary QDs obtained with $g_r=0.1$, 0.2 and 0.4 ML/s, respectively). The phosphine flux was fixed at 5 sccm. The dot densities are: (a) (2.3 ± 0.2) 10^{10} dots/cm^2, (b) (4.1 ± 0.3) 10^{10} dots/cm^2, and (c) (1.3 ± 0.1) 10^{10} dots/cm^2.

In order to better assess the morphology of this series of samples, in Fig. 6, we present the following cross-sectional micrographs: [Fig. 6(a)] sample E under DF 002 condition, [Fig. 6(b)] sample B under DF 002 condition (chemical contrast), [Fig. 6(c)] same physical region of sample B, but under BF 002 condition (strain fields, due to the contribution of the 004 reflection), and [Fig. 6(d)] sample F under DF 002 condition. We can observe that the defective island on the right-hand side of Fig. 6(b) contains dislocation lines, as shown in Fig. 6(c). By comparing Figs. 6(a) with 6(b), we can see that, within the experimental uncertainties, the coherent islands in sample E are about the same size as those in sample B (see Table II).

Figure 6(d) indicates that sample F had a much higher density of defective islands than the other samples grown at a lower g_r. As in the first series, the island dimensions of samples E and F were determined from averaging images similar to Fig. 6 and also from high-resolution micrographs (see Table II). However, as it can be seen in Fig 6(d), due to the high density of defective islands in sample F, the chemical contrast of the QDs cannot be easily discerned. In order to perform a reliable size determination for this sample, we compared the lateral diameters measured by cross-sectional TEM with those obtained from plan-view images (Fig. 5). The diameters measured by cross section are consistent provided we make the following image contrast interpretations: (i) regions with defective islands consist of those large and dark regions which extend almost to the surface [see right-hand side of Fig. 6(d)], and (ii) more localized dark regions contain defect free islands [islands are indicated by arrows in Fig. 6(d)]. The diameters are: (15 ± 3) nm, (17 ± 5) nm, and (12 ± 4) nm for samples B, E, and F, consistent with the plan-view images of Fig. 5.

[This article is copyrighted as indicated in the article. Reuse of AIP content is subject to the terms at: http://scitation.aip.org/termsconditions. Downloaded to] IP: 200.130.19.173 On: Wed, 19 Mar 2014 16:22:22

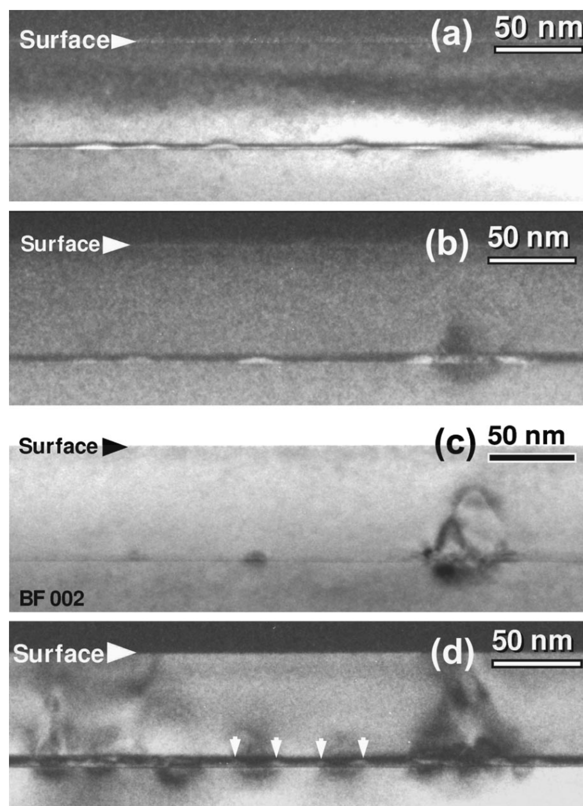

FIG. 6. (a), (b), and (d) cross-sectional TEM DF 002 micrographs of samples E, B, and F (ternary QDs obtained with $g_r = 0.1$, 0.2, and 0.4 ML/s). (c) Cross-sectional TEM BF 002 micrograph of the same area of sample B shown in (b). The phosphine flux was fixed at 5 sccm. The average dot diameters are: (a) (17 ± 5) nm, (b) (15 ± 3) nm, and (d) (12 ± 4) nm.

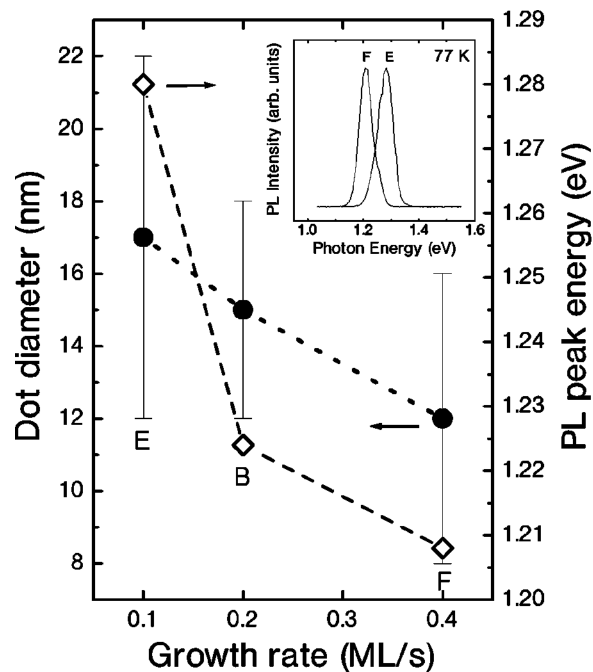

FIG. 7. Dot diameter (full circles) and PL peak energy (open diamonds) as a function of the growth rate for samples E, B, and F. Their PL spectra are shown in the inset. Lines are guides for the eyes.

Figure 7 presents a summary of TEM and PL results for samples E, B, and F, by plotting both the average island diameter (solid circles) and the PL peak energies (open diamonds) as a function of the growth rate. There is a monotonic decrease of the island diameters as g_r increases and, associated with this decrease, we also observe a redshift of the PL peak energies. This comparison leads to the conclusion that the variations obtained in the PL energies for the InAsP QDs samples (Fig. 1) are a direct consequence of a more significant As incorporation. Despite the high density of defective dots, the inset of Fig. 7 indicates the good optical quality of the samples. The PL linewidths are 70.5 meV, 60.5 meV, and 54.1 meV for samples E, B, and F.

As it was observed so far, the mechanisms involved in As incorporation are controlled mainly by varying g_r and, in a less effective way, by varying the PH_3 flux (Fig. 1). Upon increasing the growth rate, we move to a kinetically controlled regime, which basically states that thermodynamics will not prevail. The pyrolisis of PH_3 takes place at higher temperatures when compared to AsH_3. Therefore, as it has been reported in literature,[14] P incorporation in InGaAsP alloys (whether ternary or quaternary alloys) is harder to accomplish due to a lower P distribution factor. In the present case, the opposite is observed and it is most likely related to the fact that the islands are under stress, making the incorporation of As harder, as it would increase the strain. This assumption finds support on the observation that for low growth rates, which would correspond to a thermodynamic limit, As incorporation was virtually impossible. However, at higher growth rates, or in the kinetic regime, As will be incorporated more easily as the system will not have enough time to incorporate P atoms (higher pyrolisis temperature for PH_3). It must be noted that for all cases, we are under supersaturation conditions for the group-V elements. We have to make a distinction now as to which thermodynamic limit would be for the anion sublattice mixing and for island growth. Inevitably they will be different, and in fact, the latter will depend on the former. The basic distinction is made by stating that group-III element adatom concentration and surface diffusion will be the determining factor, insofar as the equilibrium size for the islands is concerned. That is not to say that at 0.4 ML/s and 550 °C we are completely under equilibrium conditions; the fact that the InAs island size decreases with the growth rate (see the blueshift of their emission energies in Fig. 1) indicates that a kinetic component is present as well.

C. High-resolution transmission electron microscopy

Now let us focus on the island morphology. Figure 8 shows high-resolution TEM micrographs of samples [Fig. 8(a)] A (InAs), [Fig. 8(b)] C (InAsP), and [Fig. 8(c)] D (InP), taken along the [110] zone axis. First, the buried InAs QDs [Fig. 8(a)] presents the not so clearly defined facets, with an aspect ratio (diameter/high) of 3.6, as can be seen in Table II. On the other hand, Fig. 8(c) shows that the InP QDs grow as a wide flat top island with an aspect ratio of 8.0. One would expect that InAsP QDs, with their lattice mismatch lying between the two binary materials, would present shapes which are also intermediate between those of Figs. 8(a) and 8(c). This can be seen in Fig. 8(b), where the InAsP QDs

[This article is copyrighted as indicated in the article. Reuse of AIP content is subject to the terms at: http://scitation.aip.org/termsconditions. Downloaded to] IP: 200.130.19.173 On: Wed, 19 Mar 2014 16:22:22

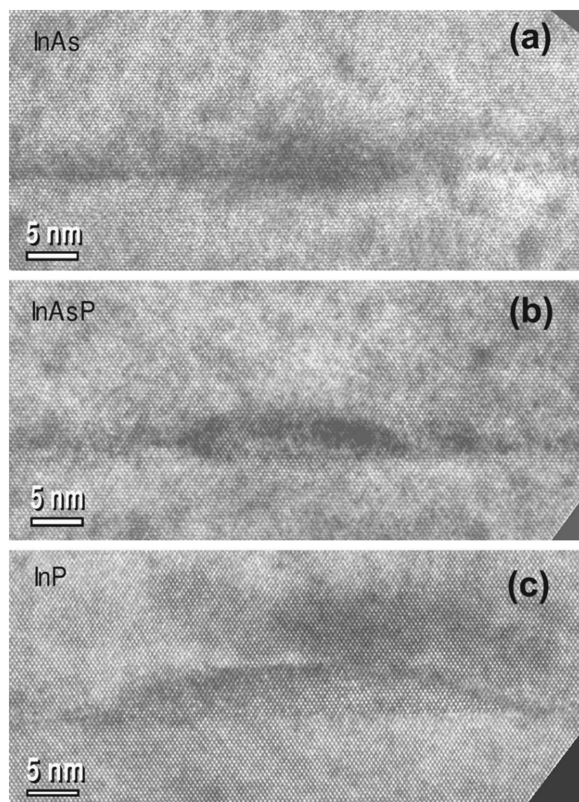

FIG. 8. High-resolution TEM images, taken along [110] zone axis, of samples (a) A (InAs), (b) C (InAsP), and (c) D (InP). The InAsP sample was obtained using a PH_3 flux of 10 sccm. All the samples were grown with $g_r = 0.2$ ML/s.

resembles a lens-shaped island, but with a slightly flattened top. The average aspect ratio of this dot is 6.9, closer to a InP-like shape. In order to conciliate the results of this structural analysis with the PL information, in Fig. 9, we plot the aspect ratio of samples A through F (see Table II) as a function of the PL peak energies. All the InAsP samples measured by TEM (different g_r and PH_3/AsH_3 flux ratios) present both an average aspect ratio and a PL peak energy which are always intermediate between the binary QDs.

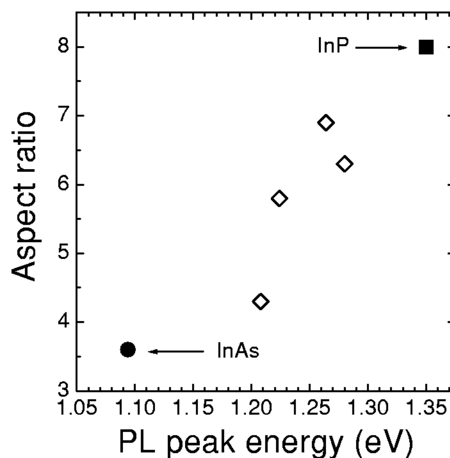

FIG. 9. Average island aspect ratio as a function of the PL peak energy for samples A through F: InAs (filled circle), InAsP (open diamonds), and InP (filled square) QDs.

IV. CONCLUSIONS

We have shown that it is possible to control the stoichiometry in the nucleation of $IIIV_xV_{1-x}$ ternary alloy QDs. The system chosen for this study was comprised of InAsP QDs embedded into GaAs, and their morphological and optical characteristics could be tailored between those of their binary constituents. By varying both the growth rate and the flux ratio PH_3/AsH_3, we were able to control the As incorporation into the alloy. It was found to be more efficient for high growth rates, when the anion sublattice mixing is driven into a kinetic regime. This is the key mechanism for changing the stoichiometry of the ternary QDs. At the thermodynamic limit ($g_r \approx 0.1$ ML/s), the stress present on these structures inhibits As incorporation. For $g_r \geqslant 0.2$ ML/s, the InAsP recombination covers the energy gap from InAs to InP QD emissions, achieving good optical quality PL spectra. As anticipated, the nucleation of defective islands took place as the amount of As incorporation increased for a fixed amount of deposited material. In summary, we were able to identify the key parameters for the nucleation of good structural and optical quality ternary alloy QDs and their corresponding shape and size evolution, and the consequences of those on the electronic properties of these nanostructures.

ACKNOWLEDGMENTS

The authors wish to thank Mr. H. Gazetta Filho for technical support with crystal growth and gratefully acknowledge financial support from LNLS, FAPESP, and CNPq-MCT.

[1] P. M. Petroff and G. Medeiros-Ribeiro, Mater. Res. Bull. **21**, 50 (1996).
[2] D. Bimberg, M. Grundmann, and N. N. Ledentsov, *Quantum Dot Heterostructures* (Wiley, Chichester, 1999).
[3] D. Leonard, M. Krishnamurthy, C. M. Reaves, S. P. Denbaars, and P. M. Petroff, Appl. Phys. Lett. **63**, 3203 (1993).
[4] R. Leon, C. Lobo, A. Clark, R. Bozek, A. Wysmolek, A. Kurpiewski, and M. Kaminska, J. Appl. Phys. **84**, 248 (1998).
[5] R. Leon, P. M. Petroff, D. Leonard, and S. Fafard, Science **267**, 1966 (1995).
[6] K. Suzuki and Y. Arakawa, Phys. Status Solidi B **224**, 139 (2001).
[7] D. A. Vinokurov, V. A. Kapitonov, O. V. Kovalenkov, D. A. Livshits, and I. S. Tarasov, Tech. Phys. Lett. **24**, 623 (1998).
[8] H. Kosaka, A. A. Kiselev, F. A. Baron, K. W. Kim, and E. Yablonovitch, Electron. Lett. **37**, 464 (2001).
[9] M. K. K. Nakaema, F. Iikawa, M. J. S. P. Brasil, E. Ribeiro, G. Medeiros-Ribeiro, W. Carvalho Jr., M. Z. Maialle, and M. H. Degani, Appl. Phys. Lett. **81**, 2743 (2002).
[10] E. Ribeiro, R. L. Maltez, W. Carvalho Jr., D. Ugarte, and G. Medeiros-Ribeiro, Appl. Phys. Lett. **81**, 2953 (2002).
[11] D. Leonard, K. Pond, and P. M. Petroff, Phys. Rev. B **50**, 11687 (1994).
[12] V. A. Shchukin, N. N. Ledentsov, P. S. Kop'ev, and D. Bimberg, Phys. Rev. Lett. **75**, 2968 (1995).
[13] F. Heinrichsdorff, A. Krost, M. Grundmann, D. Bimberg, A. Kosogov, and P. Werner, Appl. Phys. Lett. **68**, 3284 (1996).
[14] G. B. Stringfellow, *Organometallic Vapor-Phase Epitaxy* (Academic, New York, 1999).

[This article is copyrighted as indicated in the article. Reuse of AIP content is subject to the terms at: http://scitation.aip.org/termsconditions. Downloaded to] IP: 200.130.19.173 On: Wed, 19 Mar 2014 16:22:22